Depth profiling of proton exchanged $LiNbO_3$ waveguides by micro-Raman spectroscopy

Gustavo R. Paz-Pujalt and David D. Tuschel
Eastman Kodak Company, Rochester, New York 14650-2011

(Received 18 January 1993; accepted for publication 13 April 1993)

Z-cut $LiNbO_3$ wafers were proton exchanged (PE) with pyrophosphoric acid. The polished edges provided a side view of the exchanged region. The region was probed by micro-Raman spectroscopy by stepping a 488.0 nm laser at intervals as small as 0.2 μm across the edge face starting below the exchanged region and moving towards the wafer surface, thereby traversing the PE region. Profiling revealed significant changes, in the 125–800 cm^{-1} and 3200–3600 cm^{-1} frequency ranges. The PE region expanded after annealing at 300 °C indicating proton penetration into the wafer. Continued annealing resulted in the progressive recovery of spectral characteristics resembling unexchanged lithium niobate. Micro-Raman profiles provide spectroscopic information regarding which vibrational modes are affected by the exchange and the annealing processes as a function of depth.

The proton exchange (PE) process has been used extensively for the fabrication of waveguides in lithium niobate.[1] Depth profiling of proton penetration has been carried out by forward recoil spectrometry, nuclear reaction, and secondary mass spectrometry. Different orientations of lithium niobate show dissimilar degrees of proton penetration during exchange, and give rise to directional dependency of the diffusion coefficient.[2,3] Though the PE process provides a convenient way of fabricating waveguides it also poses some problems. PE waveguides suffer from index of refraction instabilities, high optical losses, and reduction in electro-optical coefficients.[4,5] Annealing at temperatures ranging from 250 to 450 °C usually results in a recovery of the electro-optic coefficients, and reduction in optical losses.[6]

Presently there is limited understanding on the effect that replacing lithium with hydrogen has on the vibrational characteristics of the lithium niobate lattice. Vibrational spectroscopic studies have been mostly limited to the OH stretching region, and to our knowledge no spatial imaging of the PE region has been reported. Naturally, optical properties are related to the structural arrangement of atoms within the exchanged layer. In fact, the physical processes accountable for Raman scattering, from modes that are also infrared active, are identical with those responsible for the electro-optic effect and, in principle, the nonlinear dielectric coefficients can be obtained from Raman measurements.[7] Lithium niobate belongs to the C_{3V} point group and has four A_1, and nine E Raman (and infrared) active transitions.

The unit cell of lithium niobate consists of two formula units. Oxygen atoms occupy the corners of octahedra with the threefold axis along the *z*-direction. Niobium and lithium atoms sit in octahedral sites with an empty site every three octahedral structures. Because of these empty sites lithium and niobium ions are shifted from the center of their corresponding octahedra. This distortion is accountable for second-harmonic generation and linear electro-optic effect.[8] The contributions of Nb—O bonds to linear and nonlinear susceptibilities is considerably more significant than that of Li—O bonds. It would be desirable to obtain vibrational spectra as a function of proton-exchange depth, and to observe how these spectra change as a function of annealing time.

The experimental procedure involved proton exchange of *z*-cut wafers with pyrophosphoric acid at 260 °C for 1 h. In order to obtain Raman spectra as a function of depth, the *x*-faces of PE wafers were polished while successively reducing the particle size of the polishing media. Approximately 2 mm of material were removed thus ensuring that the measurements probed H penetration along the *z*-axis. Figure 1 shows a photomicrograph of the *x*-face of PE lithium niobate illuminated by *z*-polarized white light. The PE region is distinguished by a section of sharp contrast at the interface. In fact, the depth of the PE region may be approximated by measuring this section.

Micro-Raman spectra depth profiles were obtained by stepping a focused 488.0 nm laser beam (~600 nm diam) at 5.0–0.2 μm increments, using an electronic stage, starting beyond the exchanged region, where the spectrum of pure lithium niobate was observed, and moving through the PE region toward the surface of the wafer. Figure 2 is a schematic of the PE wafer indicating the manner in which depth profiling was done. Differential scanning calorimetry measurements on powders and on PE wafers,

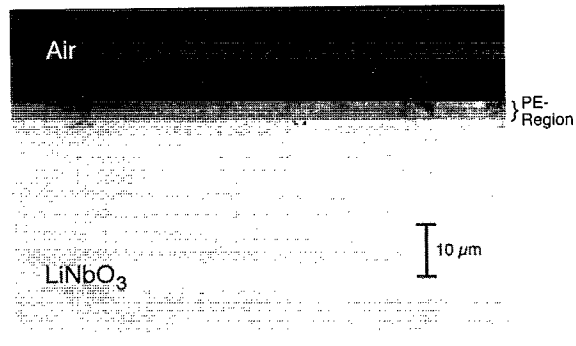

FIG. 1. *Z*-polarized light photomicrograph of proton exchanged $LiNbO_3$ viewed through the *x*-face.

 0003-6951/93/263411-03$06.00

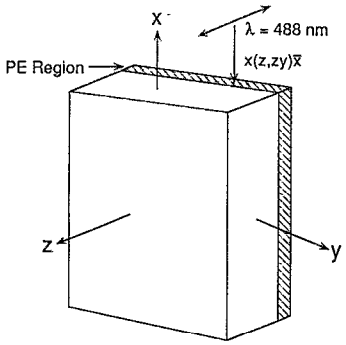

FIG. 2. Schematics of the experimental setup for micro-Raman laser depth profile imaging.

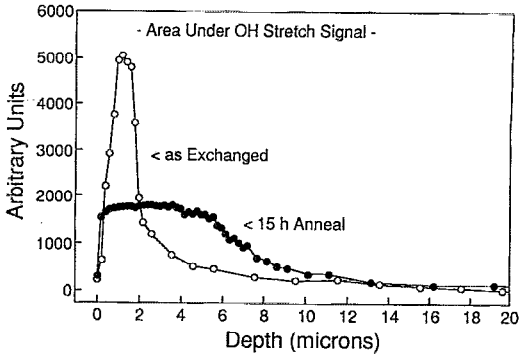

FIG. 4. Depth profile of the PE region based on the area under the OH-stretch for 1 h PE.

provided a basis for choosing the annealing temperature of 300 °C.

A series of Raman spectra from 125 to 1000 cm^{-1} along with the —OH stretch region between 3200 and 3600 cm^{-1}, plotted as a function of penetration depth, is presented in Fig. 3. The distinctness with which the PE region may be imaged is clearly noticeable. It is important to point out the absence of the broad band adjacent to the OH-stretch reported by other workers using infrared techniques.[4] The PE process reduces the scattering strengths of various modes including those responsible for nonlinear optical properties. In virgin lithium niobate, the bands between 250 and 450 cm^{-1} are related to Nb-O-octahedra bending modes, and the bands from 450 to 800 cm^{-1} are associated with Nb-O-octahedra stretching vibrations.[9,10] The most notable changes after PE are in band intensities in the 200–500 cm^{-1} region, and most importantly, the appearance of a broad band in the 650–750 cm^{-1} region. This band suggests that the distortions to the niobium octahedron have been partially removed by substitution of Li, a highly electropositive element, with the more electronegative H. Pure $HNbO_3$, a centrosymmetric material, has a band at a similar frequency suggesting that this mode originates from a paraelectric-like phase.[11] In view of this transformation it is not surprising that the PE process results in the disappearance or reduction of nonlinear coefficients. The possibility that parts of the PE layer may consist of completely substituted lithium niobate ($HNbO_3$) has been ruled out because of the absence of other characteristic Raman bands; namely in the OH stretch region. X-ray diffraction measurements do not detect the presence of this phase either.

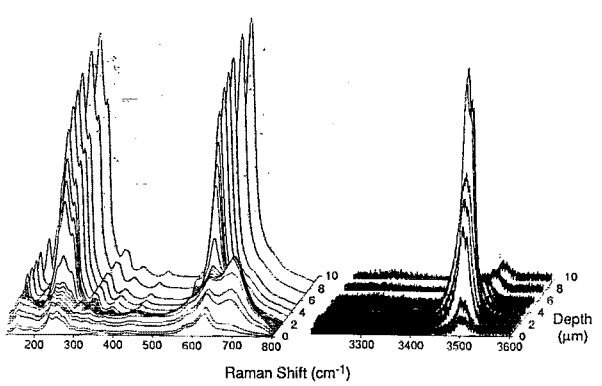

FIG. 3. Raman depth profile of 1 h PE $LiNbO_3$

Spectra closest to the surface of the PE region show intensity variations and band shifts, when compared to the rest of the PE region; these may be indicative of a thin layer of different composition. Richter and co-workers[12] have reported a very thin layer of $HNbO_3$ perovskite at the top of PE waveguides. Our results indicate that these bands to not correspond to $HNbO_3$. It is important to point out, however, that we have detected $HNbO_3$ by micro-Raman spectroscopy on rough or poorly polished $LiNbO_3$ surfaces after proton exchange with pyrophosphoric acid. In Fig. 4 the area under the OH stretch family of spectra is plotted versus depth, it provides a profile of relative proton concentration. The exchanged region has a step-like profile similar to those charted by SIMS and other techniques.[4] There is, in addition, a long tail extending deep into the wafer. The signal ultimately drops to zero indicating that the long tail is due to proton penetration and not due to intrinsic OH. The points closest to the surface of the sample indicate a layer of lower OH concentration. However, it must be remembered that peak intensities (and areas) are related to scattering efficiencies, and that these may not be comparable between the surface layer and the rest of the PE region particularly if they have a different composition and/or structure. These lower intensity bands disappear upon annealing indicating that they are not artifacts caused by the beam probing in the air-PE region interface. Also included in this figure is a depth profile of a sample annealed for 15 h at 300 °C. Exchange depths determined from micro-Raman depth profiles correspond well with those determined from the photomicrographs. These two techniques provide a simple nondestructive approach of demarcating the PE region depth.

Annealing lowers proton concentration from the exchanged region by driving protons deeper into the wafer (Fig. 4). Rice[13] identified a series of complex solid-state reactions and transformations, suggesting that the annealing process is more than reordering and removal of stress from the PE layer. A comparison of Raman spectra, taken

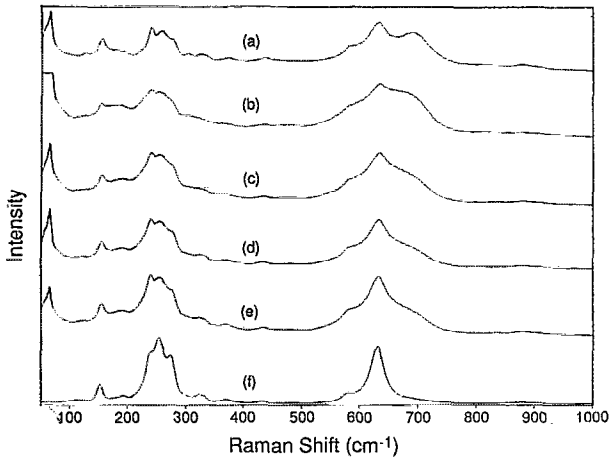

FIG. 5. Raman spectra of 1 h PE $LiNbO_3$ as a function of annealing time. (a) As-exchanged, (b) 1 h anneal, (c) 4 h anneal, (d) 10 h anneal, (e) 15 h anneal, (f) unexchanged $LiNbO_3$.

at 2.0 μm from the surface of the PE region as a function of annealing time is shown in Fig. 5. Annealing causes the band associated with PE at 690 cm^{-1} to gradually lose intensity and the Raman spectrum reverts to resemble unexchanged $LiNbO_3$. A more detailed analysis of the effects of proton exchange and annealing on the vibrational spectrum of PE $LiNbO_3$ will be presented in an upcoming publication.

In summary, micro-Raman spectroscopy provides an ideal way of nondestructively probing the width of PE waveguides. In addition vibrational information may be linked directly to properties of interest such as electro-optic and nonlinear optic coefficients. Because the nonlinear optical properties of the crystal are coupled to distortions in the Nb-O octahedra, the effects of annealing can be observed directly as a function of time by following relative intensities of the appropriate bands.

The authors acknowledge the technical help of Lillie M. Salter and Ralph Nicholas III, and valuable suggestions from: Jose M. Mir, John Agostinelli, Tom Blanton, Dilip Chatterjee, James Chwalek, Gabriel Braunstein, Mool Gupta, and Eric Lim. Kay Servais and Jill Bellucco are thanked for editing and preparing the manuscript.

[1] J. L. Jackel, C. E. Rice, and J. J. Vaselka, Appl. Phys. Lett. **41**, 607 (1982).
[2] C. Canalli, A. Carnera, G. Della Mea, P. Mazzoldi, S. M. Al Shukri, A. C. G. Nutt, and R. M. De La Rue, J. Appl. Phys. **59**, 2643 (1986).
[3] J. T. Cargo, A. J. Filo, M. C. Hughes, V. C. Kannan, F. A. Stevie, J. A. Taylor, and R. J. Holmes, J. Appl. Phys. **67**, 627 (1990).
[4] A. Loni, G. Hay, R. M. De La Rue, and J. M. Winfield, J. Lightwave Technol. **7**, 911 (1989).
[5] X. Cao, R. Srivastava, R. V. Ramaswamy, and J. Natour, IEEE Photon. Tech. Lett. **3**, 25 (1991).
[6] W. Y. Hsu, G. Braunstein, V. Gopalan, C. S. Willand, and M. C. Gupta, Appl. Phys. Lett. **61**, 3083 (1992).
[7] I. P. Kaminow, *An Introduction to Electro-Optics Devices* (Academic, New York, 1974).
[8] C. C. Shih and A. Yariv, J. Phys. C **15**, 825 (1982).
[9] S. D. Ross, J. Phys. C **3**, 1785 (1970).
[10] A. A. McConnell, J. S. Anderson, and C. N. R. Rao, Spectrochim. Acta **32A**, 1067 (1976).
[11] I. Savatinova, S. Tonchev, E. Popov, E. Liarokapis, and C. Raptis, J. Phys. D **25**, 106 (1992).
[12] R. Richter, T. Bremer, P. Hertel, and E. Kratzig, Phys. Status Solidi A **114**, 765 (1989).
[13] C. E. Rice, J. Solid State Chem. **64**, 188 (1986).